

Analysis and Behavior of Buried Culverts with Slotted Joints

MICHAEL G. KATONA and ADEL Y. AKL

ABSTRACT

Corrugated metal culverts with circumferentially slotted bolt-hole-connections, a new concept in culvert technology, have the potential to significantly reduce thrust stress (ring compression) in deep embankment installations. From a design viewpoint, this means that deeper burial depths can be achieved or lighter-gauge metal can be used or both. The results of a comprehensive investigation on the structural behavior, analysis, and design of slotted-joint culvert installations are summarized. The scope includes data gathering, experimental testing, analytical model development, verification with field data, and guidelines for design. Based on laboratory load-deformation tests, slotted-joint behavior is simulated with a five-parameter model and incorporated into the CANDE computer program with two methods for solving the culvert-soil boundary value problem: a modified elastic solution and a finite-element procedure. The latter method, which offers sophisticated modeling capabilities (e.g., incremental construction, nonlinear soil models, and frictional interfaces), is shown to correlate well with experimental field data. The former method, although more idealized, provides a keen insight into fundamental behavioral aspects of slotted-joint culverts and is an extremely useful design aid. Both analytical and experimental findings demonstrate that the slotted bolt-hole concept is extraordinarily successful in reducing ring compression. In many cases allowable fill height may be increased 40 ft or more.

Large corrugated metal culverts have dramatically increased in civil engineering use during the last two decades, and there is an increasing trend to use them in deep-fill installations; for example, burial depths well in excess of 100 ft are no longer uncommon (1). Maximum burial depths are often controlled by thrust stress (ring compression) to preclude wall or seam failure. Additional design concerns include deflection, buckling, and excessive flexural stresses or strains (2,3).

Large culverts are assembled in the field by bolting together curved, corrugated metal plates to form a particular shape (e.g., circular, elliptical, arch). In conventional practice, the longitudinal connections (seams) are friction-type lap joints with high-strength bolts tightened (torqued) to prevent joint slippage during backfilling. Backfilling with good-quality, well-compacted soil around and above the culvert is of utmost importance to the structural integrity of the installation. If the backfill is properly installed, the stiffness of the enveloping soil mass dominates the flexural stiffness of the culvert (4). Thus, soil design is the most effective way of controlling flexural distress such as ovaling deflections, outer fiber straining, and buckling (large deformations).

In contrast, however, the circumferential stiffness of the culvert dominates the corresponding soil stiffness. As a consequence, the culvert tends to attract circumferential thrust loading, that is, the negative arching effect, limiting the allowable burial depth. An innovative way to overcome this problem is to reduce the culvert's circumferential stiffness by allowing a predetermined amount of joint slippage to occur through the use of slotted bolt holes.

The concept of slotted bolt connections is simple, as may be visualized in Figure 1. Rather

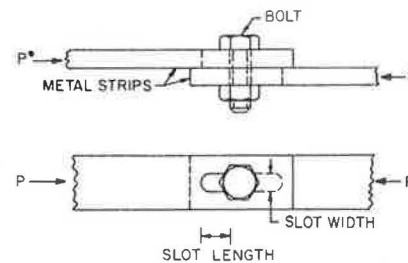


FIGURE 1 Illustration of slotted joint.

than an attempt to bolt corrugated structural plate segments into a continuous unit, the bolt holes are slotted in the circumferential direction to permit relative circumferential contraction of the plates (i.e., after the thrust force exceeds a predetermined frictional bolt clamping resistance). As the culvert circumferentially contracts from joint slippage, the surrounding soil envelope is forced into a compression arch, which in turn carries a greater portion of additional loading (i.e., positive soil arching). When all joint slippage is complete, the culvert again acts as a continuous unit so that further loading will be carried by both the structure and the soil arch. Ultimate failure in thrust typically occurs by seam failure (i.e., bearing failure), but at a burial depth significantly greater than that of a standard culvert without slotted joints.

As of this writing, there are only eight known installations that have employed this new concept; they are listed in Table 1. All of those culverts were supplied by Armco, Inc., and are circular pipes (diameters ranging from 5 to 17 ft) with 6- x 2-in.

TABLE 1 Slotted-Joint Culvert Installations

Year Completed	Location and Owner	Diameter (ft)	Gauge	Fill Cover (ft)	Comments
1975	Los Angeles, Calif.; Caltrans	10	12	188	Nonfunctional test installation, known as DB culvert test (5)
1979	Idaho; Idaho Department of Transportation	14	7	80	Bridge replacement for Rock Creek (6)
1979	Arizona; Tucson Gas and Electric Company	17	8	55	Special installation for Tucson Gas and Electric Company
1980	Utah; Utah Department of Transportation	16	8	35	Stream crossing
1981	Kentucky; Martiki Coal Company	5	1	350	Coal-mine access
1982	Kentucky; U.S. Corps of Engineers	15.5	8	55	Stream crossing
1983	Montana; Montana Department of Transportation	15	7	43	Deep Creek stream crossing (7)
1984	Montana; Montana Department of Transportation	12.5	7	75	Spring Creek stream crossing (7)

corrugated steel plates that utilize the keyhole-slot configuration (Figure 2), which provides 1 in. of slot travel per joint. The functional installations are reported to be performing properly with fill depths exceeding conventional practice. Four of these installations, most notably the nonfunctional DB (Davis-Bacher) culvert test in California, were instrumented, and the experimental data have been published (5-7).

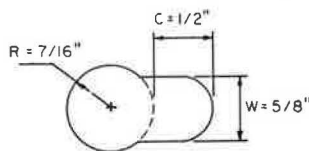


FIGURE 2 Standard keyhole slot dimensions.

OBJECTIVE

This paper is devoted to the study of the slotted bolt-hole concept applied to deeply buried, large-diameter 6- x 2-in. corrugated steel culverts. Before this study no rational theoretical or empirical method to predict the soil-structure behavior of this new concept had been offered. Such a method is needed before widespread applications of this innovative and cost-saving concept can realize its full potential. Thus, the objective is to develop reliable analytical models applicable to the design and understanding of slotted-joint culverts.

SCOPE AND APPROACH

A comprehensive step-by-step approach was undertaken to reach the objective, including gathering of data, performing experiments, formulating and verifying analytical models, and finally developing design methodologies and guidelines. The specific steps are summarized as follows:

1. Field data: Information on all known slotted-joint culvert installations was collected. Those installations with reliable experimental data were identified in order to provide a data base for subsequent analytical verification.

2. Laboratory experiments: Existing laboratory data on the load-deformation behavior of slotted joints were collected and summarized. An extensive experimental program was planned and executed to ascertain the influence of physical factors (e.g., slot width, metal thickness, bolt torque, and load eccentricity) on the load-deformation characteristics. Based on the foregoing, a five-parameter load-

deformation model (stress and strain representation) for simulating slotted-joint behavior was developed.

3. Analytical soil-structure models: Two analytical approaches for solving plane-strain, culvert-soil systems were modified to incorporate the five-parameter joint model: a closed-form elasticity solution (Burn's theory) and a finite-element solution procedure. Both methods are currently operative in the CANDE computer program (8-10).

4. Parametric studies: Parametric investigations with the analytical models include comparison of solution methods and the influence of system variables such as slotted-joint properties, pipe-soil interface friction, linear and nonlinear soil models, bedding stiffness, and metal yielding. Recommendations for modeling assumptions are discussed, and optimum slotted-joint characteristics are identified.

5. Verification with field data: Experimental data from two slotted-joint culvert installations are used to evaluate and verify the analytical model. In one case (California DB culvert), the comparison includes two similar installations, one with and one without slotted joints, which offers a direct assessment of the benefits obtained from slotted joints.

6. Design methods: Design criteria for slotted-joint culverts are established along with recommendations for system parameters. Two design methodologies are developed, one based on the finite-element method and the other on the modified elasticity solution. Although the former is more general and applicable to a wider class problem (e.g., noncircular culvert shapes), the latter is easy to use, conservative, and applicable to the majority of pipe installations. By using a conservative set of slotted-joint parameters, allowable fill-height tables are developed as a function of soil stiffness, pipe diameter, and metal thickness.

The foregoing steps are highlighted in the ensuing discussion, with emphasis on analysis and behavior (steps 1-5). Although design implications and criteria are discussed, the development and presentation of the design tables (step 6) are too lengthy to give here. They can be found in a report by Katona and Akl (8).

SLOTTED-JOINT BEHAVIOR

Experiment Tests

Figure 3 shows the load-deformation behavior of a typical slotted-joint specimen tested as a short column in uniaxial compression at Notre Dame's structural laboratory. For reference, the response of a standard (unslotted) joint specimen is also shown (11). As illustrated in the figure, the slot-

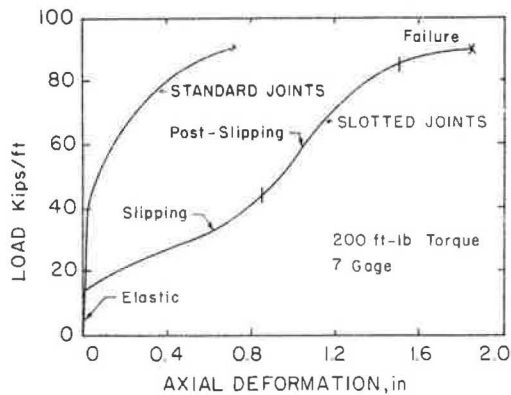


FIGURE 3 Example of joint behavior and slotted-joint zones.

ted-joint behavior is separated into four zones, the elastic zone representing the response before slippage, the slipping zone beginning when the axial load overcomes the bolt-clamping resistance and continuing until the slots are closed, the postslipping zone beginning when the bolt shank comes in contact with both ends of the slot and continuing to maximum load, and finally the failure zone representing plasticlike deformation until ultimate bearing failure.

The nature of the load-deformation response in each of the four zones is dependent on a variety of physical factors, such as bolt torque (as well as the number and size of bolts), metal thickness, slot width, slot length, and surface treatment. Based on results of pilot experimental studies by Armco, Inc. (obtained from Robert Standley, chief engineer of Armco Construction Products Division, Middletown, Ohio), an experimental program was planned and conducted at the University of Notre Dame to ascertain the influence of pertinent physical factors on the load-deformation characteristics and to develop a model simulating slotted-joint behavior.

Test specimens (supplied by Armco, Inc.) were made from two mating plates of galvanized 6- x 2-in. corrugated steel with rectangular steel plates welded to the specimen's ends to facilitate uniform loading. Assembled specimens, measuring 12 in. in width and height, were fastened with four 3/4-in. diameter bolts (4-in. lap joint) according to standard culvert practice.

Thirty-six experiments (with each experiment repeated) were performed to investigate the influence of bolt torque, loading eccentricity, metal thickness, slot width, and surface treatment. The particular example shown in Figure 3 is for 200 ft-lb bolt torque, no external moment, and 7-gauge galvanized steel with standard keyhole slot geometry. Test details and complete results are reported elsewhere (8). Here the findings are summarized in terms of an idealized model. To this end, two important experimental findings are noted. First, the degree of eccentric loading has negligible influence on the load-deformation response; that is, only the thrust load, not the external moment, influences the joint response. Second, the observed load-deformation response of all tests can be adequately modeled by four piecewise linear segments representing elastic, slipping, postslipping, and failure zones. These findings are inherent in the following model.

Stress-Strain Model

Figure 4 shows the five-parameter stress-strain idealization of slotted-joint behavior characterized

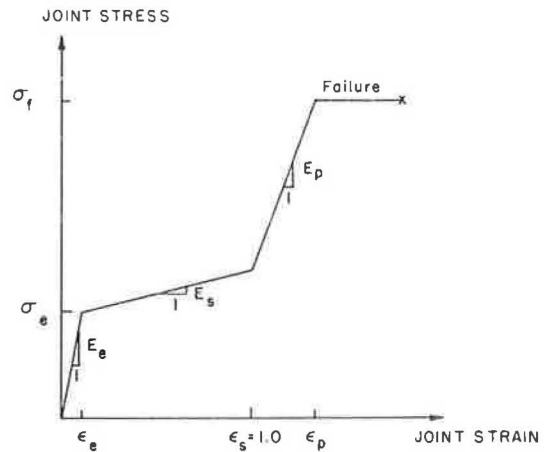


FIGURE 4 Five-parameter pseudo stress-strain model for slotted joints.

by three tangent moduli values (E_e , E_s , and E_p) representing elastic, slipping, and postslipping zones, respectively, and two stress measures (σ_e and σ_f) representing the elastic limit (or initial slipping stress) and failure stress, respectively. Of course, this is not a classical description of stress and strain. Rather, the parameters are pseudo measures of stress and strain that provide a convenient way to unify the experimental data and to facilitate model development by using the following definitions.

Joint stress is expressed as the thrust (axial load) divided by the cross-sectional area of one corrugated plate. Joint strain is expressed as the change in joint length divided by the joint length, where joint length is defined as the net slot length per joint (e.g., 1 in. for standard keyhole slots). By this definition the joint strain at the end of the slipping zone is unity ($\epsilon_s = 1.0$ in Figure 4).

With regard to the load-deformation experiments, the definition of joint strain is important because it eliminates the influence of the test specimen's length, which contains the joint length as a subcomponent. By decomposing the overall specimen deformation into joint and nonjoint contributions, the response of the joint can be isolated to get the joint's stress-strain response and hence model parameters E_e , E_s , E_p , σ_e , and σ_f (Figure 4). The mechanical process for achieving this decomposition is deferred to a later section.

To summarize, the slotted-joint stress-strain model is a piecewise linear relationship, incrementally defined by

$$\Delta\sigma = E_j \Delta\epsilon_j \quad (1)$$

where

- $\Delta\sigma$ = increment of thrust stress,
- $\Delta\epsilon_j$ = corresponding increment of joint strain, and
- E_j = current joint modulus dependent on the zone of loading.

That is, E_j is defined in four loading zones by

$$E_j = \begin{cases} E_e = \text{initial elastic modulus} & 0 \leq \epsilon_j < \epsilon_e \\ E_s = \text{slipping modulus} & \epsilon_e \leq \epsilon_j < \epsilon_s \\ E_p = \text{postslipping modulus} & \epsilon_s \leq \epsilon_j < \epsilon_p \\ E_f = 0 \text{ (failure zone)} & \epsilon_p \leq \epsilon_j \end{cases} \quad (2)$$

where the zone strain limits are inherently determined by the five model parameters. Because this paper is only concerned with monotonic loading, unloading characteristics are not addressed.

As reasonably expected, the elastic joint modulus E_e was found to be equivalent to the elastic modulus of steel (i.e., $E_e = 30 \times 10^6$ psi) in all tests. By using this fixed value for E_e , the ratios E_s/E_e and E_p/E_e describe the remaining joint moduli values in a convenient nondimensional form. Similarly, by using the yield stress of steel as reference ($\sigma_y = 33,000$ psi), the ratios σ_e/σ_y and σ_f/σ_y describe nondimensional initial slipping stress and joint failure stress, respectively. In Table 2 the experimental values of these four ratios and their correlation to physical factors are summarized. As will be shown, the slipping modulus E_s is an important parameter and must be sufficiently low if the full benefit of slotted-joint culverts is to be achieved.

TABLE 2 Experimental Values of Joint Stress-Strain Parameters

Joint Parameters ^a	Typical Value ^b	Range of Values ^c	Comments and Observations
σ_e/σ_y	0.15	0.06-0.30	Primarily influenced by bolt torque; increasing bolt torque linearly increases σ_e
E_s/E_e	0.0003	0.00015-0.0004	Primarily influenced by slot width; increasing slot width slightly decreases E_s
E_p/E_e	0.0024	0.0006-0.003	Erratic variation with all physical factors (high values are recommended)
σ_f/σ_y	1.0	0.85-1.05	Consistent values not significantly influenced by physical factors; light gauges have lower σ_f

^aReference parameters, $E_e = 30 \times 10^6$ psi, $\sigma_y = 33,000$ psi.

^bTypical value is for 7-gauge galvanized steel with standard keyhole slots and 200 ft-lb bolt torque.

^cVariations in physical factors: metal thickness = 10-, 7-, and 1-gauge; bolt torque = 100, 200, and 400 ft-lb; slot width = 5/8, 11/16, and 3/4 in.; surface treatment = galvanized steel with and without various coatings.

SOIL-STRUCTURE ANALYTICAL MODELS

Two previously established solution approaches for soil-culvert systems are used as a starting point for incorporating the slotted-joint stress-strain model: an elasticity model with a closed-form solution presented by Burns (12) and a general finite-element procedure contained in the CANDE program (9,10). Both approaches assume plane strain geometry and small-deformation theory. Of course, the finite-element approach provides a great deal more modeling flexibility (e.g., incremental construction, nonlinear soil models, and arbitrary culvert shapes); however, the elasticity solution offers a keen insight into the soil-structure behavior, and its application to design is quite remarkable.

The modification of these solution methods for simulating slotted-joint behavior is accomplished by special treatment of the culvert's circumferential stiffness (tangent modulus) as a function of thrust loading (Equations 1 and 2). For Burns' solution the slotted joints are assumed to be uniformly smeared around the circumference, whereas in the finite-element solution slotted joints are modeled locally by special beam-column elements. Each approach is discussed in turn.

Modified Elasticity Approach

Burns' theory, as originally presented, provides an exact solution of an elastic, circular pipe encased

in an isotropic, homogeneous, infinite elastic material (soil) with a uniformly distributed overburden pressure acting on a horizontal plane far above the pipe. Thin-shell theory is assumed for the pipe and continuum elastic theory is employed for the surrounding soil. Two solutions are offered depending on the pipe-soil interface assumption—completely bonded or frictionless (no interface shear stress).

Table 3 summarizes Burns' solutions for the key responses of the pipe for both interface assumptions. However, the solutions presented are cast in a different notation from that originally presented by Burns. Two dimensionless parameters are introduced (α and β), defined as follows:

$$\alpha = EA/2GR \quad (\text{relative circumferential stiffness}) \quad (3)$$

$$\beta = EI/2GR^3 \quad (\text{relative flexural stiffness}) \quad (4)$$

Here, α is the ratio of the pipe's circumferential stiffness EA to a corresponding measure of circumferential soil stiffness, where G is the soil shear modulus and R is the pipe radius. Similarly, β is a ratio of the pipe's flexural stiffness to a measure of flexural soil stiffness. It is interesting to note that for typical pipe-soil systems (without slotted joints), $\alpha \gg 1$ and $\beta \ll 1$. In other words, circumferential stiffness is dominated by the pipe, and flexural stiffness is dominated by the soil, as discussed in the introduction. To illustrate the use of the table, the thrust force at $\theta = 45$ degrees is $N = P_0 R \alpha / (1 + \alpha)$ for both interface conditions.

In adapting the elasticity solutions to simulate slotted-joint behavior, the equations are applied in an incremental fashion to accommodate changes in the circumferential stiffness (E^*A) as overburden pressure increases. E^*A , which is a smeared average of the elastic pipe wall and all slotted joints, has four possible values corresponding to the four zones of slotted-joint behavior. Initially E^* is the elastic steel modulus E_e . When the average thrust stress exceeds σ_e (initial slipping stress), E^* is reduced to represent joint slipping (shown subsequently) and this value is retained until the total circumferential contraction of the pipe is equal to the sum of all slot lengths. On further loading, E^* is increased to represent postslipping until the average thrust stress reaches σ_f (joint failure), after which the incremental modulus is zero.

In the development of the expression for E^* , the geometric ratio

$$J_r = C_{\max}/2\pi R \quad (5)$$

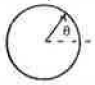
is used, where C_{\max} is the sum of all slot lengths. Thus, J_r is the fraction of the pipe's circumference containing slots. With the foregoing, E^* is given by

$$E^* = E_j / [(1 - J_r)E_j/E_e + J_r] \quad (6)$$

where E_j is the load-dependent joint modulus (Equation 2) and E_e is the elastic steel modulus (note that if $E_j = E_e$ or $J_r = 0$, $E^* = E_e$).

The derivation of Equation 6 is based on the smeared-joint approximation. That is, any differential segment of the pipe's circumference (s) is assumed to be composed of two subparts, a joint portion ($s_j = J_r s$) and an elastic, pipe-wall portion ($s_e = (1 - J_r)s$). By taking the modulus of the joint portion as E_j and the elastic portion as E_e , the net effective modulus E^* for the differential segment can be determined as given by Equation 6.

TABLE 3 Elasticity Solution Equations for Key Pipe Responses for Bonded and Frictionless Interfaces

Structural Response of pipe	Common Factor Defining Units	Bonded Interface	Frictionless Interface
		$A^* = (1+K) + 3(5-K)\beta + (3+K)\alpha + 12(3-K)\alpha\beta$	$A^* = (1+K) + 3(5-K)\beta$
Radial Pressure on Pipe P_r	P_0	$\alpha/(1+\alpha) - \{(1-K)(-2\alpha+18\beta+24\alpha\beta)/A^*\}\cos 2\theta$	$\alpha/(1+\alpha) - [18(1-K)\beta/A^*]\cos 2\theta$
Tang. Pressure on Pipe P_θ	P_0	$\{(1-K)(4\alpha+24\alpha\beta)/A^*\}\sin 2\theta$	0.0
Radial Disp. of Pipe w	$P_0 \frac{R(1-K)}{2G}$	$1/[(1-K)(1+\alpha) - \{(2+4\alpha)/A^*\}\cos 2\theta]$	$1/[(1-K)(1+\alpha) - \{2/A^*\}\cos 2\theta]$
Tang. Disp. of Pipe v	$P_0 \frac{R(1-K)}{2G}$	$\{(2+2\alpha+6\beta)/A^*\}\sin 2\theta$	$\{1/A^*\}\sin 2\theta$
Moment in Pipe Wall M	$P_0 R^2$	$\beta/(1+\alpha) + \{(6\beta(1-K)+12\alpha\beta(1-K))/A^*\}\cos 2\theta$	$\beta/(1+\alpha) + \{6(1-K)\beta/A^*\}\cos 2\theta$
Thrust in Pipe Wall N	$P_0 R$	$\alpha/(1+\alpha) + \{(1-K)(2\alpha+6\beta+24\alpha\beta)/A^*\}\cos 2\theta$	$\alpha/(1+\alpha) + \{6(1-K)\beta/A^*\}\cos 2\theta$
Shear Resultant in Pipe Q	$P_0 R$	$\{(1-K)(-12\beta-24\alpha\beta)/A^*\}\sin 2\theta$	$\{-12(1-K)\beta/A^*\}\sin 2\theta$

Note: Soil properties are as follows: G = shear modulus, K = lateral pressure coefficient [related to Poisson ratio by $K = \nu_s/(1 - \nu_s)$], P_0 = overburden pressure. Pipe properties are as follows: E = plane-strain Young's modulus [defined by $E = E_{\text{steel}}/(1 - \nu^2)$], I = moment of inertia, A = thrust area, R = average radius. Dimensionless parameters are $\alpha = EA/2GR$ and $\beta = EI/2GR^3$.

To summarize, increments of overburden pressure are prescribed, and incremental responses (e.g., thrusts, moments, displacements) are computed from Table 3 by using the current value of E^* to define α (β remains constant). The incremental responses are summed into running totals to give the net response values throughout the loading schedule.

Finite-Element Approach

The finite-element formulation in the CANDE program is well documented elsewhere (9,10,13). Some program features applicable to this study include incremental construction; pipe-soil interface friction elements; continuum soil elements with several constitutive models, including Duncan's hyperbolic model (14); and beam-column elements with material nonlinearity for modeling the culvert. The so-called level 2 option of CANDE provides an automated mesh generation scheme, whereas the level 3 option is for special culvert installations requiring a user-defined mesh (the level 1 option employs Burns' elasticity solution).

The finite-element treatment of slotted-joint behavior described here is similar to the approach used in the elasticity solution but without the global joint-smearing approximation. Rather, standard beam-column elements are defined locally at each joint location, and the current axial stiffness E^*A of each element is computed based on its individual load-deformation history. Two types of joint elements are considered, a matched joint element and an imbedded joint element. In the former the element length exactly matches the actual joint length (e.g., 1 in.), in which case E^* is identical to value to E_j (Equation 2). An imbedded joint element is a longer element containing the joint length as a subcomponent, that is, a local joint smearing. Accordingly, E^* is determined from Equation 6 except that J_r is redefined as the ratio of joint length to element length. Imbedded joint elements have the computational advantage of maintaining uniform element spacing around the pipe's circumference without an excessive number of elements.

Solutions are obtained by applying load increments, that is, soil layers or pressure increments

or both. For each increment, the current value of E^*A is individually assigned to the axial stiffness of each joint element, but bending stiffness is not altered by joint action. Iterations within the load step are employed to accommodate cornering transitions of E^* from one zone to the next (8).

BEHAVIOR OF IDEALIZED SOIL-STRUCTURE MODELS

A small sampling of the parametric studies conducted during the course of this investigation is presented here to compare and contrast solution methods and to illustrate the behavior of slotted-joint culverts for various modeling assumptions.

To begin, consider the idealized pipe-soil system shown in Figure 5, which assumes a frictionless interface. This is a monolith system with increments of overburden pressure for which the elasticity approach would provide an exact solution in the absence of slotted joints. By introducing the discrete slotted joints into the system, the validity of the joint-smearing approximation can be assessed by comparing results with those from the finite-element solution employing matched joint elements. Similarly, the validity of the imbedded joint elements can be assessed.

Both finite-element mesh configurations in the immediate vicinity of the pipe are shown as inserts in Figure 5, taking advantage of biaxial symmetry. (It is important to remember that a frictionless pipe-soil interface is assumed in this example.)

Figures 6, 7, and 8 show key pipe responses (thrust, deformations, and moments) as functions of overburden loading for slotted and unslotted pipes. In each figure, overburden pressure is represented by fill height through the relationship $H = P/\gamma$ and nondimensionalized by the pipe radius.

These results illustrate the remarkable agreement among the solution methods, thereby lending credence to the joint-smearing approximation, both globally (elasticity solution) and locally (imbedded joint element solution). In addition, these results provide a fundamental understanding of slotted-pipe behavior contrasted with that of unslotted pipes.

Consider, for example, Figure 6, which shows maximum thrust (springline) nondimensionalized by

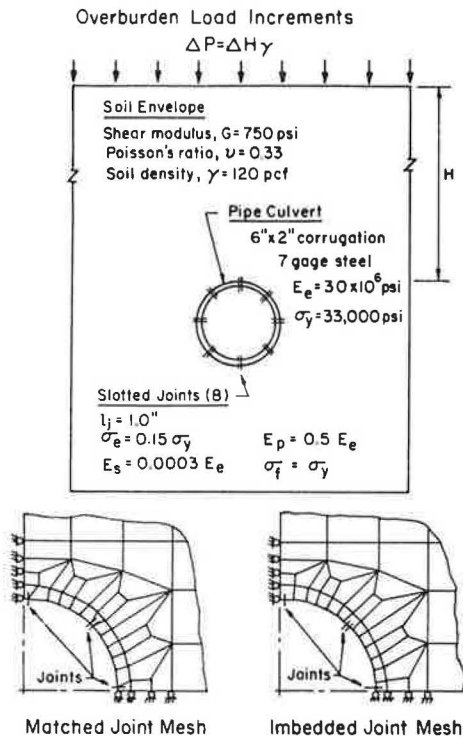


FIGURE 5 Idealized model and local finite-element-method modeling.

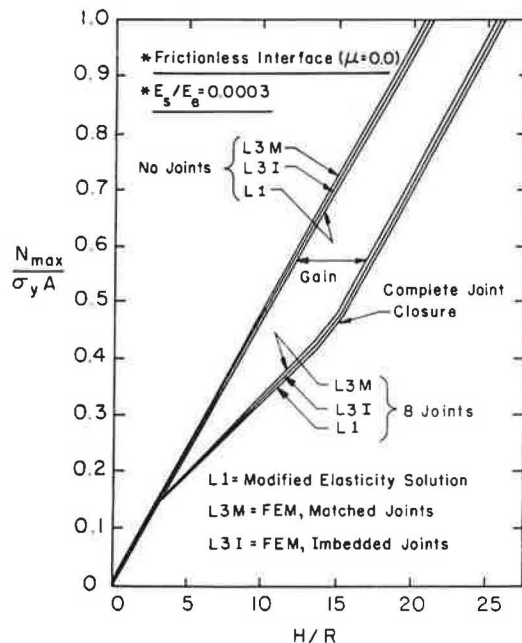


FIGURE 6 Comparison of solution methods for slotted-joint effect on maximum thrust.

the steel yield strength. If the allowable thrust stress is specified as one-half of the yield stress (ignoring other design criteria for the time being), the slotted pipe can safely withstand an increase in burial depth of approximately five radii beyond that of the unslotted pipe, a gain of 60 ft in this example.

With regard to deformations, Figure 7 shows that the slotted pipe exhibits an increase in vertical flattening and a decrease in horizontal elongation

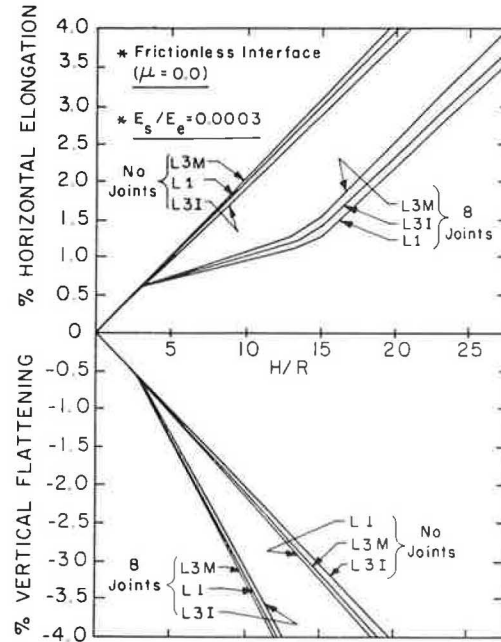


FIGURE 7 Comparison of solution methods for slotted-joint effect on pipe deformations.

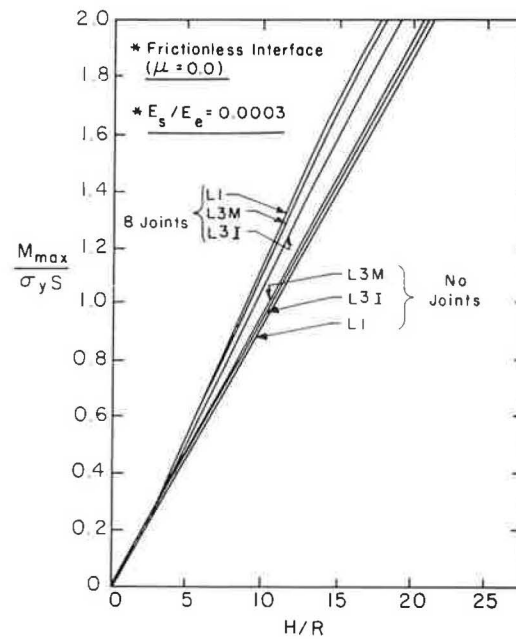


FIGURE 8 Comparison of solution methods for slotted-joint effect on maximum bending moment.

as compared with the unslotted pipe. Such deformation behavior is easily explained as the superposition of flexural ovaling and uniform circumferential contraction due to slot closure. Thus, the increase in vertical flattening is not considered a shortcoming for slotted pipes because only ovaling deformation is of design concern. If circumferential contraction is disregarded, the slotted pipe's ovaling deformation is similar to that of the unslotted pipe. The conventional 5 percent allowable ovaling deformation is recommended for design of slotted and unslotted pipes.

Maximum moments, shown in Figure 8 and nondimensionalized by the yield moment, are slightly in-

creased by the introduction of slotted joints. Outer fiber yielding is tolerated (indeed, expected) for deeply buried pipes and is commonly ignored. However, for slotted pipes it is recommended that outer fiber flexural strain be limited to no more than twice the value of yield strain. Even so, thrust stress is usually found to be the controlling design criterion, not flexural strain or ovaling deformations.

Next, the importance of the joint-slipping modulus (E_s) is illustrated by considering three parametric values, $E_s/E_e = 1, 3$, and 6×10^{-4} ; all other parameters remain as in the previous example. Figure 9 shows how the thrust response is influenced by E_s (for clarity, only the results from the finite-element solution with matched joint elements are shown; the other solution methods produced nearly identical results). In the absence of a design limit on maximum thrust, it was observed that all three slotted pipes would eventually provide the same fill-height gain with respect to the unslotted pipe. However, when the design limit is enforced (i.e., one-half yield stress), it can be seen that the full potential gain cannot be realized unless, in this example, E_s/E_e is approximately less than 3×10^{-4} .

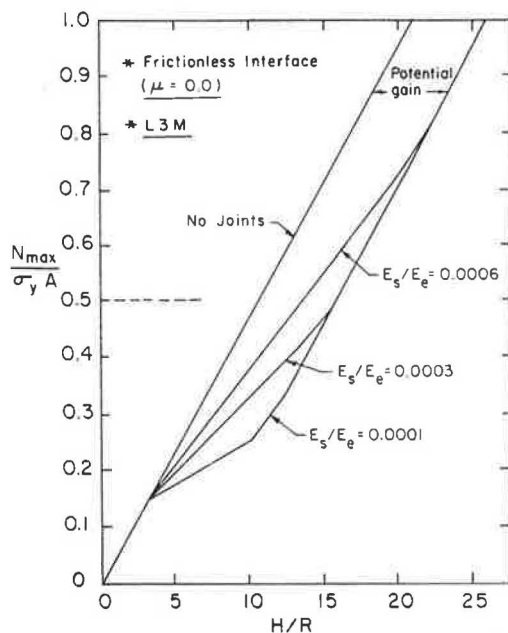


FIGURE 9 Effect of joint modulus ratio on maximum thrust.

By using the foregoing concept of fill-height gain, the modified elasticity equations can be manipulated to give a general expression for potential fill-height gain, valid for any set of system parameters:

$$H_{\text{gain}} = 2G J_r (1 - E_s/E_e) / \gamma \quad (7)$$

This simple yet rather remarkable result shows that the full gain is directly proportional to the soil shear modulus (G) and the ratio of all slot lengths to pipe circumference (J_r). However, whether the full gain can be realized depends on whether complete joint slippage can be achieved before any design criterion is exceeded.

For the specific example defined in Figure 5, the influence of friction at the pipe-soil interface is

considered next. Typically, the interface friction coefficient between steel and soil is in the range 0.1 to 0.5. However, if a completely bonded condition is assumed (infinite coefficient of friction), it may be seen in Figure 10 that the finite-element solution with matched joints (dashed line) differs from the other two solutions (imbedded joint solution and the modified elasticity solution), both of which are similar and employ a joint-smearing approximation.

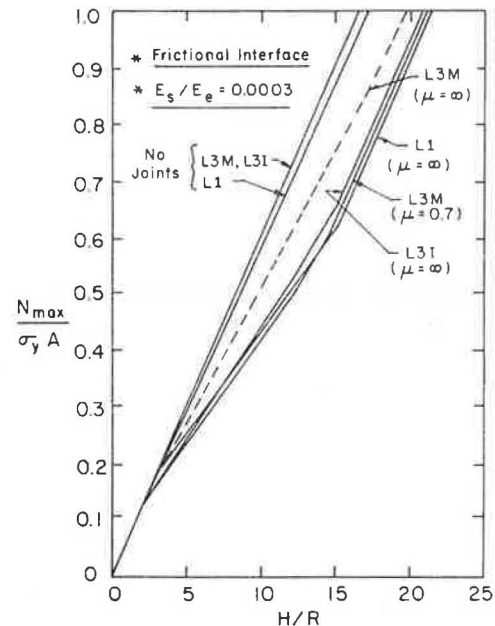


FIGURE 10 Comparison of solution methods for slotted-joint effect on maximum thrust.

Theoretically, the matched joint element solution is more correct, but realistically it is not. This is because the matched joint element contracts over a small local area (1 in.), and because of the assumption of complete bonding, the soil is locally "pinched," which creates an extremely high concentration of interface shear traction that far exceeds any reasonable value of frictional resistance. In contrast, the solution methods with joint-smearing approximations spread the shear traction over substantially greater lengths, which reduces the shear traction intensity to values that could be reasonably sustained across an actual soil-structure interface. To demonstrate, when the finite-element models are re-solved by using a friction coefficient of 0.7 (considered by the authors as a realistic upper bound), the solutions for the unslotted pipe remain the same. Also, the imbedded joint solution is practically unchanged; that is, it remains effectively bonded. However, the matched joint solution does change, because of local release of high shear traction, and conforms with the bonded imbedded joint solution shown in Figure 10 (solid line). It was concluded that the solution methods are in good agreement for any interface assumption, frictionless to effectively bonded, with a proviso that for matched joint models, effective bonding means that there is an upper bound for the friction coefficient, say 0.7.

The influence of interface friction on the slotted-pipe behavior can be assessed by considering the two extreme conditions, frictionless (Figure 6) and effectively bonded (Figure 10), which bracket all

intermediate conditions. For the bonded condition the thrust increases at a rate approximately 25 percent greater than that of the frictionless condition throughout the loading history for both the slotted and the unslotted pipe. Hence, even though the potential fill-height gain is the same for both interface conditions, the bonded condition induces a proportionately larger net thrust into the slotted and unslotted pipe. In contrast, however, moments and deformations are proportionately reduced by the bonded assumption, but only on the order of 10 percent (not shown).

Insights from these idealized examples are extremely useful for interpreting the subsequent results in which more sophisticated finite-element models with incremental construction and hyperbolic soil models are used to simulate actual field experiments.

COMPARISON WITH FIELD DATA

Experimental data from two separate slotted-pipe installations, the DB test culvert in California (5) and the Spring Creek installation in Montana (7), are used to evaluate and verify the finite-element model. Although the two installations differ in scale, burial depth, number of joints, and soil properties, the basic mesh topology and loading scheme, as shown in Figure 11 (CANDE level 2), is applicable to both installations. With an assumption of vertical symmetry, 10 uniformly spaced beam-column elements are used to model one-half of the pipe's circumference, which infers that imbedded joint elements are employed where applicable. The initial configuration includes the pipe, in situ soil, bedding, and fill soil to the springline level. Four gravity construction increments are used to raise the fill soil to three radii above the crown; thereafter surface pressure increments are applied to represent overburden loadings. Temporary surcharge pressures of 5 psi are used to simulate compaction effects for the intermediate construction layers up to the crown level.

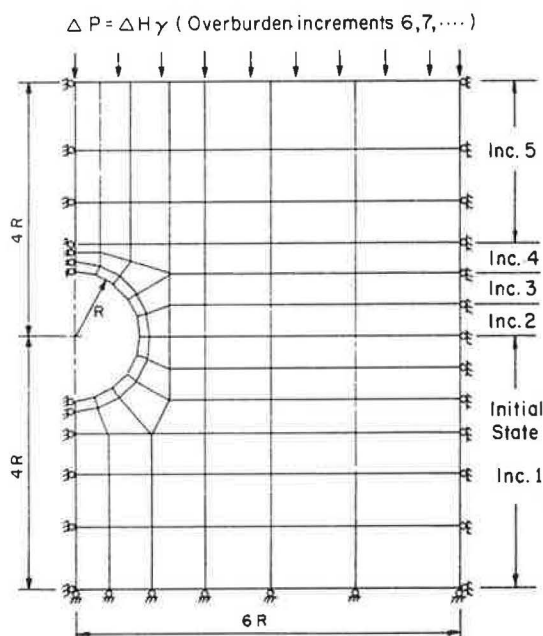


FIGURE 11 Finite-element-method representation of California and Montana installations with imbedded joint elements.

With the general modeling scheme described in the foregoing, each installation is specialized by identifying an appropriate set of system dimensions and parameters to obtain numerical solutions. Springline thrust and pipe deformations as a function of fill height are used to compare predictions with field performance. These responses provide an excellent assessment of structural distress modes (thrust and flexure) throughout the loading history and also show initiation and completion of joint slippage. As soil-structure analysts know, the adequate prediction of these responses by any analytical model is an exceedingly difficult task. The prediction is dependent not only on the general formulation but also on the detailed information of system parameters. Parameter identification and assumptions are discussed in turn for each installation along with the comparative results.

California DB Culvert

Figure 12 is a schematic view of a 10-ft-diameter slotted-pipe installation designated Zone 6 in the thoroughly instrumented, nonfunctional DB experimental test conducted by the California Department of Transportation (5). Overall, the experiment included eight separate zones, one of which, Zone 4, is similar to Zone 6 except that standard joints are used. Thus, the data from these two zones provide a unique opportunity to compare slotted-pipe performance directly with that of a corresponding unslotted pipe as well as evaluate the finite-element models.

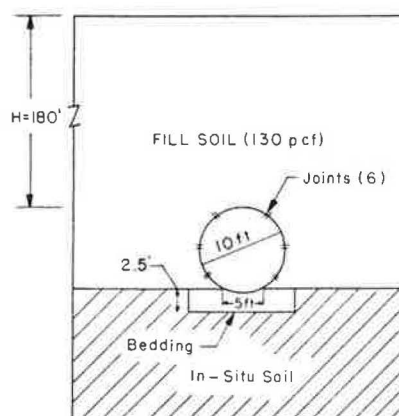


FIGURE 12 Embankment configurations of DB culvert Zones 4 and 6.

The pipes in both test zones are formed from six 12-gauge, 6- x 2-in. corrugated steel plates (i.e., six joints) and were loaded to and beyond seam failure in a deep embankment installation.

Except for the modeling of joints, the remaining system parameters are assumed to be identical for both test zones, as listed in Table 4 and explained in the following. Backfill soil, described as a silty sand compacted to 90 percent relative density, and the granular bedding material exhibited similar behavior in laboratory triaxial test experiments. Accordingly, a common hyperbolic soil model (Duncan) is used for both bedding and backfill. The hyperbolic parameters listed in Table 4 are adopted from a previous model-fitting study of triaxial data from soil samples taken from Zone 4 (15). Fill-soil density is 130 pcf. In situ soil is assumed linear elastic, and the pipe-soil interface friction coef-

TABLE 4 System Parameters for DB Culvert, Zones 4 and 6

Parameter	Formula
Pipe (12-gauge steel)	
Young's modulus	$E_e = 30 \times 10^6$ psi
Yield stress	$\sigma_y = 33,000$ psi
Cross-sectional area	$A = 0.1296$ in ² /in.
Moment of inertia	$I = 0.0604$ in ⁴ /in.
Fill soil and bedding, Duncan hyperbolic (15)	
Friction angle	$\phi_0 = 43$ degrees
Reduction in friction angle	$\Delta\phi_0 = 10.6$ degrees
Cohesion intercept	$C = 0$
Modulus number	$K = 600$
Modulus exponent	$n = 0.47$
Failure ratio	$R_f = 0.80$
Bulk modulus ratio	$K_b = 325$
Bulk modulus exponent	$m = 0$
In situ soil, elastic	
Young's modulus	$E = 2,000$ psi
Poisson's ratio	$\nu = 0.4$
Pipe-soil interface friction coefficient	$\mu = 0.1$
Joint properties, Zone 6 (Zone 4)	
Joint length	$l_j = 1.0$ in. (0.125)
Initial slipping stress	$\sigma_s = 3,000$ psi (9,000)
Joint failure stress	$\sigma_f = 2,500$ psi (2,500)
Slipping modulus	$E_s = 6,000$ psi (750)
Postslipping modulus	$E_p = 30,000$ psi (3,750)

efficient is taken as 0.1 based on engineering judgment and numerical experimentation.

For Zone 6, the joint parameters listed in Table 4 are in conformance with the Notre Dame slotted-joint experiments, except for the initial slipping stress, which is specified as lower than normal. This is because special fixed-grip bolts (i.e., partially threaded) were used with the keyhole slots, which did not provide sufficient clamping force and resulted in some premature joint slippage. (Standard bolts have been used in all subsequent keyhole slot installations.) With regard to Zone 4, a miniature 1/8 in. slot length is used to simulate the behavior of a standard joint, where 1/8 in. represents small gaps between bolt holes and shanks. Selection of the remaining standard joint parameters, noted parenthetically in Table 4, was guided by engineering judgment and numerical experimentation.

Figure 13 shows springline thrust versus fill height above crown level for Zones 4 and 6 as pre-

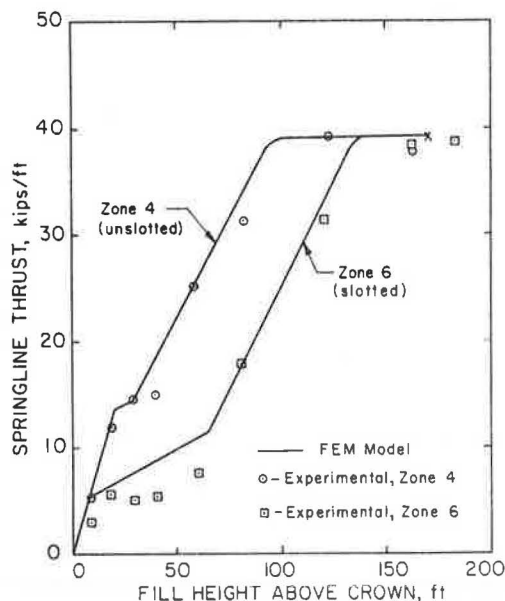


FIGURE 13 Thrust versus fill height for Zones 4 and 6, DB culvert.

dicted by the finite-element model and as experimentally measured by using the average value of four pairs of strain gauges located near the springlines. Complete joint closure for Zone 6 is predicted at 65 ft of fill, which is nearly identical to the experimentally recorded value of 63 ft. Overall, model predictions are in good agreement with measured values, including the miniature sliplike behavior of Zone 4. A minor discrepancy is observed during the joint-slipping phase for Zone 6, where measured thrust values are somewhat lower than predicted, most likely caused by premature joint slippage because of partially threaded bolts.

If the relative performance between Zones 4 and 6 is compared, both predictive and experimental results indicate a fill-height gain of approximately 40 ft for the slotted-pipe installation based on an allowable thrust limit of, say, one-half of the ultimate.

Horizontal elongation and vertical flattening for both zones are shown in Figure 14. Again, the predicted responses correlate well with the experimental trends, especially with regard to the relative performance of the two zones. Zone 6 (slotted joints) exhibits significantly less horizontal elongation but greater vertical flattening than Zone 4 (standard joints). As previously explained with the idealized examples, the increase in vertical flattening is simply a consequence of circumferential contraction of the slotted joints and need not be a design limitation.

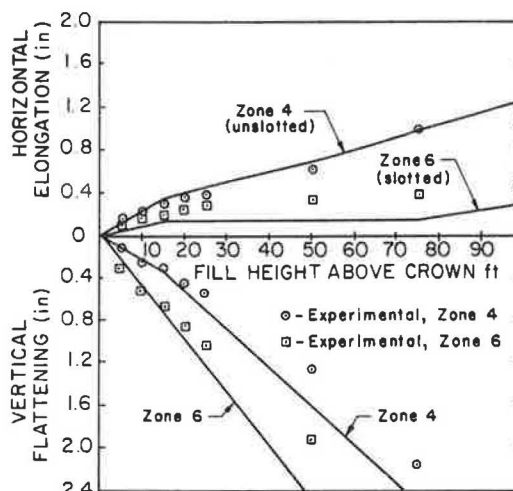


FIGURE 14 Horizontal elongation and vertical flattening versus fill height for Zones 4 and 6, DB culvert.

Montana Spring Creek Installation

Figure 15 shows a schematic view of a functional, 12.5-ft-diameter pipe with eight keyhole joints installed in a deep embankment (75 ft of cover) to provide a highway crossing over Spring Creek in Montana. Experimental data, including strain gauge data and deformations, were reported by the Montana Department of Highways (8) up to 63 ft of cover.

Table 5 summarizes the system parameters for the finite-element model based on the following assumptions. Both backfill and bedding are reported as sandy silt to silty sand gravel compacted to 90 percent relative density. Because no triaxial test data are available, the hyperbolic parameters are patterned after a standard value for Duncan's SM-90 soil classification with a density of 130 pcf. In

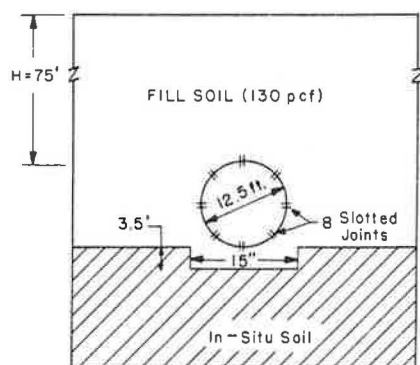


FIGURE 15 Embankment configurations of Montana Spring Creek.

TABLE 5 System Parameters for Montana Spring Creek Installation

Parameter	Formula
Pipe (7-gauge steel)	
Young's modulus	$E_p = 30 \times 10^6$ psi
Yield stress	$\sigma_y = 33,000$ psi
Cross-sectional area	$A = 0.2283$ in ² /in.
Moment of inertia	$I = 0.1080$ in ⁴ /in.
Fill soil and bedding, Duncan hyperbolic (15)	
Friction angle	$\phi_0 = 32$ degrees
Reduction in friction angle	$\Delta\phi_0 = 4$ degrees
Cohesion intercept	$C = 0$
Modulus number	$K = 500$
Modulus exponent	$n = 0.25$
Failure ratio	$R_f = 0.70$
Bulk modulus ratio	$K_b = 400$
Bulk modulus exponent	$m = 0$
In situ soil, elastic	
Young's modulus	$E = 2,000$ psi
Poisson's ratio	$\nu = 0.4$
Pipe-soil interface friction coefficient	$\mu = 0.1$
Joint properties (keyhole slots) ^a	
Joint length	$l_j = 1.0$ in.
Initial slipping stress	$\sigma_e = 5,500$ psi
Joint failure stress	$\sigma_f = 5,100$ psi

^a E_p and σ_f are not activated.

situ soil and interface friction is assumed as in the previous study, and slotted-joint parameters are representative of standard keyhole slots. Note, however, that the postslipping modulus and joint failure stress are not activated for the design loading.

Experimental and predicted values of average thrust stress versus cover height, shown in Figure 16, are in good agreement. (Note that experimental data were reported as an average thrust strain from seven strain gauges located at middepth of the corrugation and spaced around the circumference.) At 63 ft of fill the springline slots were reported to be approximately 60 percent closed, which compares favorably with 70 percent for the predicted value. A potential fill-height gain of more than 50 ft, as compared with that for an equivalent joint-slipping modulus is projected for this installation.

Horizontal elongation, averaged from the measurements of two stations, is shown in Figure 17 along with predicted values. Again, good agreement is observed. It is interesting to note the reversal of outward movement that occurs when joint slipping begins at approximately 15 ft of fill above the crown.

CONCLUSIONS AND RECOMMENDATIONS

Analysis and experiments show that a slotted-joint culvert experiences significantly less thrust stress

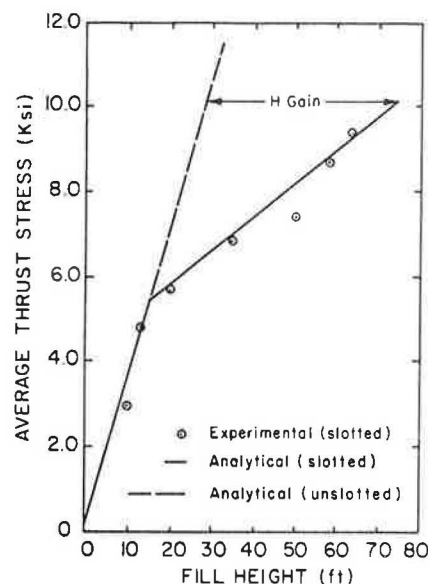


FIGURE 16 Average thrust versus fill height for Montana Spring Creek.

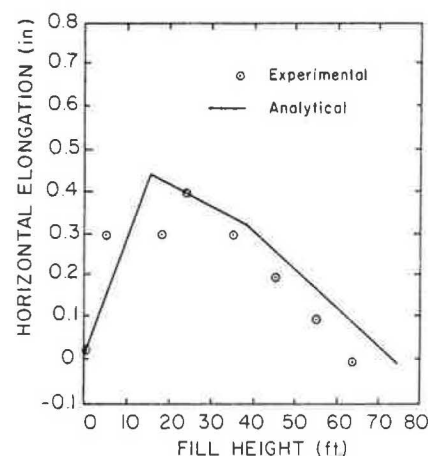


FIGURE 17 Horizontal elongation versus fill height for Montana Spring Creek.

in deep embankment installations than the same culvert with standard bolted joints. Accordingly, a deeper burial depth (e.g., a fill-height gain of about 50 ft) can be achieved at little or no expense by using slotted bolt holes. The potential fill-height gain is proportional to the net length of all slots and the soil shear modulus (Equation 7). In order to realize this full potential gain, thrust stress must be the controlling design criterion, which is usually the case when good quality backfill soil is used. Also, the so-called joint-slipping modulus must be sufficiently small in relation to the elastic steel modulus, say, $E_s/E_e < 0.0003$.

Results from soil-structure finite-element models that used a five-parameter stress-strain representation to simulate slotted-joint behavior correlated very well with experimental data from two slotted-joint culvert installations, including a cross-check comparison of a standard-joint culvert installation. Also, the modified elasticity solution, although not as sophisticated in modeling capabilities, predicts thrusts, moments, and displacements in excellent agreement with idealized finite-element models for both frictionless and bonded pipe-soil interface

conditions. Extensive parameter studies have revealed that in addition to providing a keen insight into slotted-joint behavior, the modified elasticity solution is an excellent design aid.

Both solution methods are currently available in the CANDE program. Input instructions are provided elsewhere along with design criteria, guidelines, and tables (8).

ACKNOWLEDGMENT

Deep appreciation is extended to the Federal Highway Administration and to George (Pat) Ring III and Roy Trent, Project Technical Managers, for supporting this work effort and providing helpful guidance. Thanks are extended to Robert Standley and Richard Lautensleger of Armco, Inc., for supplying information and test specimens along with valuable expertise and experience on slotted-joint culverts.

REFERENCES

1. E.T. Selig, J.F. Able, F.H. Kulhawy, and W.E. Falby. Review of the Design and Construction of Long-Span, Corrugated-Metal, Buried Conduits. Technical Report. FHWA, U.S. Department of Transportation, Oct. 1977.
2. Standard Specifications for Highway Bridges, 12th ed. AASHTO, Washington, D.C., 1977.
3. Handbook of Steel Drainage and Highway Construction Products, 2nd ed. American Iron and Steel Institute, Washington, D.C., 1971.
4. M.G. Katona et al. Structural Evaluation of New Concepts for Long-Span Culverts. Report FHWA-RD-79-115. FHWA, U.S. Department of Transportation, 1979, 286 pp.
5. Prooftesting of a Structural Plate Pipe with Varying Bedding and Backfill Parameters, Sections II, III, and VIII. Interim Draft Reports FHWA/CA/SD-81/07 and FHWA/CA/SD-82/10. FHWA, U.S. Department of Transportation, 1981-1982.
6. W.E. Meritt and L.E. Van Over. Yielding Seam Multi-Plate Pipe. Idaho Transportation Department, Boise, Aug. 1980.
7. Preliminary Report on Instrumentation of Two Key-Slot Pipes on the Shirley West Interstate Project. Montana Department of Highways, Helena, Dec. 1983.
8. M.G. Katona and A.Y. Akl. Metal Culverts with Slotted Bolt Holes. FHWA, U.S. Department of Transportation, Aug. 1984.
9. M.G. Katona et al. CANDE: A Modern Approach for the Structural Design of Buried Pipe Culvert. Report FHWA-RD-77-5. FHWA, U.S. Department of Transportation, Oct. 1976, 475 pp.
10. M.G. Katona et al. Box Culverts and Soil Models. Report FHWA-RD-80-172. FHWA, U.S. Department of Transportation, May 1981, 210 pp.
11. C.D. Arrand. A Study of the Properties of Corrugated Metal Pipe Joints Subject to Compression and Bending. Report EES 279-1. Ohio State University, Columbus, Feb. 1968.
12. J.Q. Burns. Analysis of Circular Cylindrical Shells Embedded in Elastic Media. Ph.D. thesis. University of Arizona, Tucson, 1965.
13. M.G. Katona. CANDE: A Versatile Soil-Structure Design and Analysis Computer Program. Journal of Advances in Engineering Software, Vol. 1, No. 1, 1978, pp. 3-9.
14. J.M. Duncan et al. Strength, Stress-Strain and Bulk Modulus Parameters for Finite Element Analyses of Stresses and Movements in Soil Masses. Report UCB/GT/78-02. National Science Foundation, Washington, D.C., April 1978.
15. C.-H. Lee. Evaluation of Duncan's Hyperbolic Soil Model. Master's thesis. University of Notre Dame, Notre Dame, Ind., May 1979.

Publication of this paper sponsored by Committee on Subsurface Soil-Structure Interaction.